

# We are IntechOpen, the world's leading publisher of Open Access books Built by scientists, for scientists

6,900

Open access books available

186,000

International authors and editors

200M

Downloads

Our authors are among the

154

Countries delivered to

TOP 1%

most cited scientists

12.2%

Contributors from top 500 universities



WEB OF SCIENCE™

Selection of our books indexed in the Book Citation Index  
in Web of Science™ Core Collection (BKCI)

Interested in publishing with us?  
Contact [book.department@intechopen.com](mailto:book.department@intechopen.com)

Numbers displayed above are based on latest data collected.  
For more information visit [www.intechopen.com](http://www.intechopen.com)



# Oceanic Evaporation: Trends and Variability

Long S. Chiu<sup>1</sup>, Si Gao<sup>1</sup> and Chung-Lin Shie<sup>2</sup>

<sup>1</sup>*Department of Atmospheric, Oceanic and Earth Sciences, George Mason University*

<sup>2</sup>*UMBC/JCET, NASA/GSFC  
USA*

## 1. Introduction

The global water and energy cycles are strongly coupled as two essential components of earth system. They play important roles in altering the Earth's climate.

Oceanic evaporation, or sea surface latent heat flux (LHF) divided by latent heat of vaporization ( $L_v$ ), is a key component of global water and energy cycle. In a bulk aerodynamic formulation, it is determined by the transfer coefficient of evaporation,  $C_E$ , and bulk parameters such as surface wind speed ( $U$ ), surface saturated and near-surface air specific humidity ( $Q_s$  and  $Q_a$ ),

$$LHF = \rho L_v C_E U (Q_s - Q_a) \quad (1)$$

where sea surface saturated humidity is determined by sea surface temperature (SST) and salinity, and  $\rho$  is density of moist air. The transfer coefficient is dependent on the stability of the atmosphere and the sea state (Liu et al., 1979; Zeng et al., 1988). Historically, marine surface observations have provided the basis for estimating these oceanic turbulent fluxes (e.g. Bunker, 1976; Cayan, 1992; da Silva et al., 1994; Esbensen & Kushnir, 1981; Hastenrath, 1980; Hsiung, 1985; Isemer & Hasse, 1985, 1987; Josey et al., 1998; Oberhuber, 1988; Renfrew et al., 2002; Weare et al., 1981). The advent of remote sensing techniques offers means to retrieve a number of surface bulk variables. Microwave radiation interacts directly with water molecules and hence is effective in providing water vapor information. The sea surface emissivity is affected by the sea state and foam conditions, which is related to surface wind. For instance, global microwave measurement of the Special Sensor Microwave Imager (SSM/I) on board a series of Defense Meteorological Satellite Program (DMSP) satellites has been used to retrieve near-surface air humidity and winds over the ocean.

At present there are several remote sensing products of global ocean surface latent heat flux. They include the NASA/Goddard Satellite-based Surface Turbulent Flux (GSSTF) dataset version 1 (Chou et al., 1997) and version 2 (GSSTF2, Chou et al., 2003), the Japanese Ocean Flux utilizing Remote Sensing Observations (J-OFURO) dataset (Kubota et al., 2002) and the Hamburg Ocean Atmosphere Parameters and Fluxes from Satellite (HOAPS) dataset (Grassl et al., 2000). Chiu et al. (2008) examined "trends" and variations in these global oceanic evaporation products for the period 1988–2000. They found a long-term increase in global average LHF that started around 1990 in GSSTF2. They argued that the dominant patterns may be related to an enhancement of Hadley circulation and El Niño-Southern Oscillation

(ENSO), respectively. An updated version of SSM/I version 6 (V6) data released by Remote Sensing Systems (RSS) in 2006 [as used by Wentz et al. (2007), see <http://www.ssmi.com>] that calibrates all SSM/I sensors is available in 2008. Shie et al. (2009) have reprocessed and forward processed GSSTF2 to version 2b (GSSTF2b, Shie et al. 2010; Shie 2010) using the SSM/I V6 data (including total precipitable water, brightness temperature, and wind speed retrieval), covering the period July 1987–December 2008. We provide an assessment of these data products and examine their “trends” and variability.

The data and methodology are described in Section 2. Section 3 presents the trends of these products, compares GSSTF2 and GSSTF2b for the pre 2000 periods, assesses the post 2000 performance, and examines the GSSTF2b Set1 and Set2 differences. Summary and discussion are presented in Section 4.

## 2. Data and methodology

Earlier version of these flux products have been described elsewhere (Chiu et al., 2008). The product versions described here represent the most updated versions as of the writing of this report.

### 2.1 HOAPS

Detail descriptions of the latest version of HOAPS, (version 3, or HOAPS-3) are given in Andersson et al. (2010). Bulk variables are derived from SSM/I data except for the SST which is derived from the Advanced Very High Resolution Radiometer (AVHRR) Oceans Pathfinder SST product. A neural network algorithm is used to derive  $U$ . The  $Q_a$  is obtained using the linear relationship of Bentamy et al. (2003). The  $Q_s$  is computed from the AVHRR SST using the Magnus formula (Murray, 1967) with a constant salinity correction factor of 0.98. The near-surface air temperature ( $T_a$ ) is estimated from the SST using the assumptions of 80% constant relative humidity and a constant surface-air temperature difference of 1 K. Latent and sensible heat fluxes are calculated using the Coupled Ocean–Atmosphere Response Experiment (COARE) 2.6a bulk algorithm (Fairall et al., 1996, 2003).

The HOAPS-3 data sets cover the time period from July 1987 to December 2005. HOAPS-G pentad and monthly data sets with 0.5-degree resolution and HOAPS-C twice daily data set with 1-degree resolution are available at the website (<http://www.hoaps.zmaw.de>).

### 2.2 J-OFURO

The updated version of J-OFURO, (version 2, J-OFURO2) is described in Tomita et al. (2010). Bulk variables  $U$ ,  $Q_a$  and SST ( $Q_s$ ) are determined by multi-satellite and multiple satellite sensors.  $U$  is obtained from a combination of microwave radiometers (SSM/I, AMSR-E and TMI) and scatterometers (ERS-1, ERS-2 and QuikSCAT).  $Q_a$  is derived from SSM/I measurements. SST is taken from the Merged satellite and in-situ data Global Daily SST (MGDSST, Sakurai et al. 2005) analysis provided by Japanese Meteorological Agency (JMA).  $T_a$  is obtained from NCEP/DOE reanalysis. COARE 3.0 bulk algorithm (Fairall et al., 2003) is used to estimate LHF and SHF. The J-OFURO2 covers the time period from January 1988 to December 2006. Daily and monthly means with 1-degree resolution are available at the website (<http://dtsv.scc.u-tokai.ac.jp/j-ofuro>).







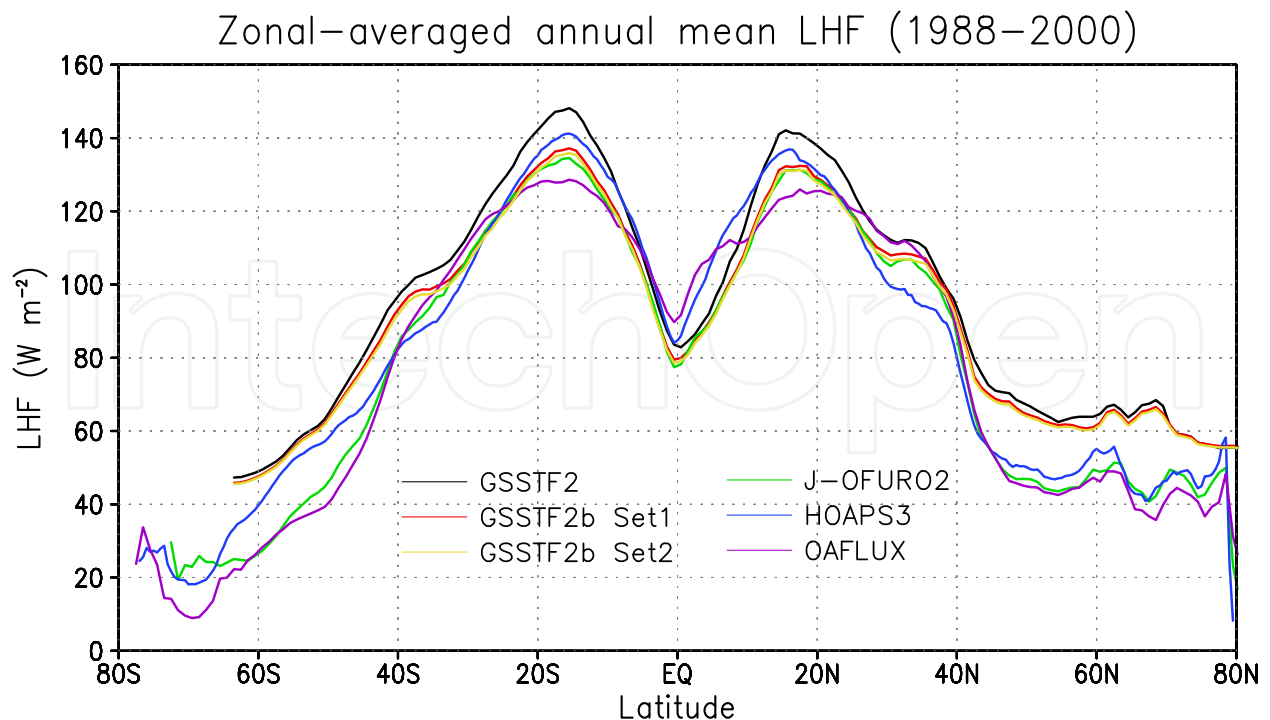


Fig. 2. Zonal annual mean of LHF for oceanic evaporation computed from HOAPS3, J-OFURO2, GSSTF2, GSSTF2b Set1 and Set2 and OAFLUX.

GSSTF2b Set2 is slightly lower than HOAPS3 but higher than J-OFURO2 and OAFLUX at their maxima. Poleward of 30°, the GSSTF zonal means are generally higher than the other products.

### 3.2 Trend analysis

Linear regression analyses of the time series with time were performed on the global mean time series. The significance of the slopes of the regression (trend) is tested using a t-test. The degree of freedom for the significance test takes into account the serial correlation of the time series (Angell, 1981; Chiu & Newell, 1983). GSSTF2 shows the largest trend. It is followed by GSSTF2b Set1 while the GSSTF2b Set2 trend is comparable to HOAPS3 and J-OFURO2 for the period of overlap (1988–2005). OAFLUX exhibits the smallest trend. Table 2 summarizes our results.

To map out the geographic differences, Figure 3 compares the spatial distribution of linear trends of GSSTF2b Set1 and Set2, HOAPS3, J-OFURO2 and OAFLUX. The linear trends are calculated for the common time period 1988–2005. While the magnitudes of the trends are different, the locations of maximum change are similar among HOAPS3, J-OFURO2 and GSSTF2b Set1 and Set2 - all show increasing trends in the storm tracks in the north Atlantic and north Pacific, the oceanic dry zones off the Inter-tropical Convergence Zone (ITCZ) in the western south Pacific and in latitude bands between 30–40°S off the coast of Australia and in the Indian Ocean. OAFLUX shows increasing trends in the storm tracks in both the North Atlantic and North Pacific, and in the eastern coastal regions off South America and Australia. There are large areas showing a decrease, notably in the south Indian Ocean, tropical eastern North Pacific and in North Atlantic.

Period	GSSTF2	GSSTF2b Set1	GSSTF2b Set2	HOAPS3	J-OFURO2	OAFUX
1988-2000	10.44	9.88	5.98	7.75	6.51	3.71
1988-2005	N/A	11.69	6.34	7.35	7.62	2.41
1988-2008	N/A	10.45	7.08	N/A	N/A	1.50

Table 2. Linear trends of LHF products (in  $W\ m^{-2}\ decade^{-1}$ ) for the different periods. All values are significant at 99% level.

